

Loop induced decays of the Little Higgs: $H \rightarrow gg, \gamma\gamma$

Tao Han, Heather E. Logan, Bob McElrath, and Lian-Tao Wang*

*Department of Physics, University of Wisconsin,
1150 University Avenue, Madison, WI 53706*

Abstract

We analyze the loop induced decays of the Higgs boson into pairs of gluons and photons in the Littlest Higgs model. We find that the deviation of the partial widths for these decays relative to their Standard Model values scales with $1/f^2$, where $f \sim \text{TeV}$ is the mass scale of the new heavy particles in the model. For $f = 1 \text{ TeV}$, $\Gamma(H \rightarrow gg)$ is reduced by 6 – 10% and $\Gamma(H \rightarrow \gamma\gamma)$ is reduced by 5 – 7% compared to their Standard Model values. While the LHC and a linear e^+e^- collider would be sensitive to these deviations only for relatively low values of $f \lesssim 650 \text{ GeV}$, a photon collider could probe the deviation in $\Gamma(H \rightarrow \gamma\gamma)$ up to $f \lesssim 1.1 \text{ (0.7) TeV}$ at the 2 (5) σ level.

* han@pheno.physics.wisc.edu
logan@pheno.physics.wisc.edu
mcelrath@pheno.physics.wisc.edu
liantaow@pheno.physics.wisc.edu

I. INTRODUCTION

The Standard Model (SM) of the strong and electroweak interactions has passed stringent tests up to the highest energies accessible today. The precision electroweak data [1] prefer the existence of a light Higgs boson of mass $m_H \lesssim 204$ GeV at 95% C.L. The Standard Model with a light Higgs boson can be viewed as an effective theory valid to a much higher energy scale Λ , possibly all the way to the Planck scale. However, without protection by a symmetry, the Higgs mass is quadratically sensitive to quantum corrections, rendering the theory with $m_H \ll \Lambda$ rather unnatural.

Little Higgs models [2, 3] revive an old idea to keep the Higgs boson naturally light. The key idea is to make the Higgs particle a pseudo-Goldstone boson of some broken global symmetry. Electroweak symmetry breaking is then triggered by a Coleman-Weinberg [4] potential, generated by integrating out heavy degrees of freedom. The Higgs boson acquires a mass at the electroweak scale possibly by radiative corrections. The Littlest Higgs (LH) model [3] is a minimal model of this type. It contains the minimal matter content necessary to accomplish the goal of canceling the Higgs mass quadratic divergence to one loop order. It consists of an $SU(5)$ non-linear σ -model which is broken down to $SO(5)$ by a vacuum condensate f . The gauged subgroup $[SU(2) \times U(1)]^2$ is broken at the same time to its diagonal subgroup $SU(2) \times U(1)$ identified as the SM electroweak gauge group. A vector-like “top quark” is also needed. Particles of the *same* spin cancel quadratic divergences among themselves.

Due to the symmetry breaking by the vacuum condensate, the theory has a natural cutoff $\Lambda \approx 4\pi f$ that is $\mathcal{O}(10 \text{ TeV})$. The new heavy states, such as the new gauge bosons, heavy vector-like quark, and scalars all have masses of the order f , naturally in the TeV range. The effects due to the new states at low energies have been studied recently and generic constraints on the model parameters, in particular f , are obtained [5, 6, 7] based on the precision electroweak measurements. Signatures for the new states at future colliders have also been examined [6, 7, 8].

In this paper, we study the loop-induced decays $H \rightarrow gg$ and $H \rightarrow \gamma\gamma$ in the Littlest Higgs model. There are several motivations to perform this study. First, while the Higgs boson is the central issue of the little Higgs models, its properties have not been carefully studied to compare with the SM expectations. By construction, the Higgs boson interactions are necessarily extended and modified beyond the SM. Second, although the new states in the LH model could be too heavy to be copiously produced at the LHC and quite possibly beyond the direct reach of a linear collider, quantum corrections due to these states running in the loops may reveal an earlier signature. Third, these loop-induced decays depend primarily on the couplings of the Higgs boson to the heavy quarks and gauge bosons, which are fixed and characteristic in the LH model. This is in contrast to the Higgs boson couplings to the light fermions, which could in principle be generated by some higher-dimensional operators, leading to model dependent uncertainties. Finally, both of these processes are finite at the one-loop order and therefore independent of the detailed physics at the cutoff scale Λ , leading to robust predictions.

It is well known that in the Standard Model, the contribution of a heavy SM particle to the loop amplitude for $H \rightarrow gg$ or $H \rightarrow \gamma\gamma$ approaches a nonzero constant value for particle masses much heavier than H (for example, this is a reasonably good approximation for the top quark loop [9, 10]). This “non-decoupling” behavior occurs because the masses of the SM particles are generated by their coupling to H , so that the mass dependence of the coupling cancels the mass dependence of the loop integral. The heavy particles in the LH model, on the other hand, get their masses from the f condensate, so that their couplings to H are not proportional to

their masses. Thus the heavy particle contributions to $H \rightarrow gg$ and $H \rightarrow \gamma\gamma$ decouple as f grows. We will show, in fact, that the deviation of these partial widths from their SM values scales with $1/f^2$.

In the next section we lay out the masses and couplings of the particles in the LH model relevant to our calculation. In Sec. III we present our results for $H \rightarrow gg$ and $H \rightarrow \gamma\gamma$, including their dependence on the additional free parameters in the LH model, and discuss the expected experimental sensitivity to these loop-induced couplings at future colliders. In Sec. IV we discuss the robustness of our results under extensions of the LH model and summarize our conclusions. Finally, we present some details of the Higgs sector necessary for our calculation in the Appendix.

II. HIGGS BOSON COUPLINGS TO NEW HEAVY STATES

Any colored fermion that couples to the Higgs boson significantly will contribute to the decay $H \rightarrow gg$. Similarly, any charged particle that couples to the Higgs boson will contribute to $H \rightarrow \gamma\gamma$. Those states in the Littlest Higgs model include the heavy $SU(2)$ gauge boson W_H^\pm , the vector-like quark T , and the charged scalars $\Phi^\pm, \Phi^{\pm\pm}$. Besides the common condensate f as the most important scale parameter, the mass and couplings for each new state depend upon additional dimensionless parameters. The mixing between the two gauge groups $SU(2)_1$ and $SU(2)_2$, with couplings g_1 and g_2 respectively, is parameterized by c . The mixing between the top quark and the heavy vector-like quark T is parameterized by c_t . In the Higgs sector, we introduce a parameter x to parameterize the ratio of the triplet and doublet vevs (v'/v). More explicitly, we have

$$0 < c = \frac{g_1}{\sqrt{g_1^2 + g_2^2}} < 1, \quad 0 < c_t = \frac{\lambda_1}{\sqrt{\lambda_1^2 + \lambda_2^2}} < 1, \quad 0 \leq x = \frac{4fv'}{v^2} < 1. \quad (1)$$

For the parameters, the electroweak data prefers a small c [5, 6], while the positivity of the heavy Higgs boson mass requires $v'/v < v/4f$, *i.e.*, $x < 1$. One should note that $x = 0$ can be achieved by tuning the contribution of the heavy vector-like quark to the Coleman-Weinberg potential against the contribution from the heavy gauge bosons to make the coefficient $\lambda_{h\phi h}$ in Eq. (A2) vanish.

The masses of the particles that run in the triangle loop diagrams are given to leading order in v/f by

$$\begin{aligned} M_{W_L}^2 &= m_w^2 \left[1 - \frac{v^2}{f^2} \left(\frac{1}{6} + \frac{1}{4}(c^2 - s^2)^2 - \frac{x^2}{4} \right) \right], \\ M_{W_H}^2 &= m_w^2 \frac{f^2}{s^2 c^2 v^2}, \quad M_T = f \sqrt{\lambda_1^2 + \lambda_2^2} = \frac{m_t}{s_t c_t} \frac{f}{v}, \\ M_\Phi^2 &= \frac{2m_H^2 f^2}{v^2} \frac{1}{[1 - (4v'f/v^2)^2]} = \frac{2m_H^2}{(1 - x^2)} \frac{f^2}{v^2}, \end{aligned} \quad (2)$$

where $m_w = gv/2$, $s^2 = 1 - c^2$, and $s_t^2 = 1 - c_t^2$. The dependence of these masses on the parameters c, c_t and x for various representative values of m_H can be seen in Fig. 1.

In general, all masses that originate with the Standard Model Higgs mechanism and all couplings to H are modified in the LH model at order v^2/f^2 . We parameterize this by the

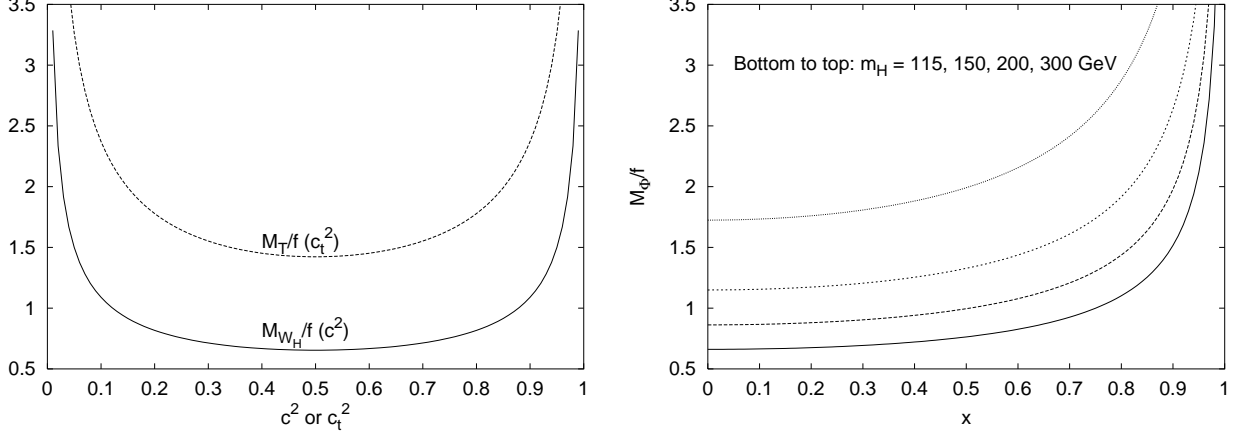


FIG. 1: (left) M_{W_H}/f as a function of c^2 and M_T/f as a function of c_t^2 ; (right) M_ϕ/f as a function of x for various values of the H mass.

factors y_i , which are the couplings of H to the particle in the loop normalized according to the form of the SM Lagrangian as follows [11, 12]

$$\begin{aligned} \mathcal{L} = & -\frac{m_t}{v} y_t \bar{t} t H - \frac{M_T}{v} y_T \bar{T} T H + 2 \frac{M_{W_L}^2}{v} y_{W_L} W_L^+ W_L^- H + 2 \frac{M_{W_H}^2}{v} y_{W_H} W_H^+ W_H^- H \\ & - 2 \frac{M_\Phi^2}{v} y_{\Phi^+} \Phi^+ \Phi^- H - 2 \frac{M_\Phi^2}{v} y_{\Phi^{++}} \Phi^{++} \Phi^{--} H. \end{aligned} \quad (3)$$

These y_i factors are derived from the Higgs couplings given in Appendix A of Ref. [7]; the Higgs self-coupling factors y_{Φ^+} and $y_{\Phi^{++}}$ are derived in the Appendix. They are

$$\begin{aligned} y_t &= 1 + \frac{v^2}{f^2} \left[-\frac{2}{3} + \frac{1}{2}x - \frac{1}{4}x^2 + c_t^2 s_t^2 \right] & y_T &= -c_t^2 s_t^2 \frac{v^2}{f^2} \\ y_{W_L} &= 1 + \frac{v^2}{f^2} \left[-\frac{1}{6} - \frac{1}{4}(c^2 - s^2)^2 \right] & y_{W_H} &= -s^2 c^2 \frac{v^2}{f^2} = -M_{W_L}^2/M_{W_H}^2 \\ y_{\Phi^+} &= \frac{v^2}{f^2} \left[-\frac{1}{3} + \frac{1}{4}x^2 \right] & y_{\Phi^{++}} &= \frac{v^2}{f^2} \mathcal{O} \left(\frac{x^2 v^2}{16 f^2}, \frac{1}{16 \pi^2} \right). \end{aligned} \quad (4)$$

For y_{W_L} we include the correction to the relation between M_{W_L} and $gv/2$. One may naively expect some sizable contribution to $H \rightarrow \gamma\gamma$ from the doubly-charged states $\Phi^{\pm\pm}$ due to the $Q^2 = 4$ enhancement of the amplitude. However, the $H\Phi^{++}\Phi^{--}$ coupling is very small, as shown in the Appendix, leading to $y_{\Phi^{++}} \sim v^4/f^4$. The doubly-charged triplet states thus do not give a significant contribution to the amplitude and we will neglect them from now on.

In the SM, the v -dependence can be traded for the precisely measured G_F . In the Littlest Higgs model, however, the relation between G_F and v is modified from its SM form, introducing an additional correction y_{G_F} as

$$\frac{1}{v^2} = \sqrt{2} G_F y_{G_F}^2, \quad \text{where} \quad y_{G_F}^2 = 1 + \frac{v^2}{f^2} \left[-\frac{5}{12} + \frac{1}{4}x^2 \right]. \quad (5)$$

This correction must also be taken into account when comparing H decay rates in the LH model to the SM predictions with G_F as input. Note that $y_{G_F}^2 < 1$ for $0 \leq x < 1$, which tends to suppress the H decay rates. For a fixed value of f , only three parameters of the Littlest Higgs model affect the loop-induced Higgs partial widths: c , c_t and x .

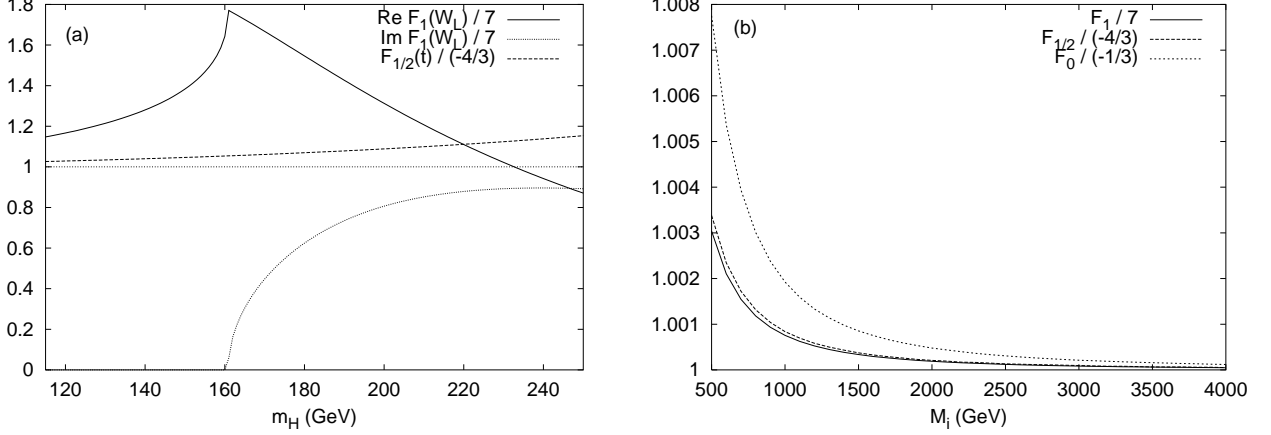


FIG. 2: (a) The loop functions $F_1(\tau_{W_L})$ and $F_{1/2}(\tau_t)$ as a function of m_H ; (b) The loop functions as a function of the heavy mass M_i , for $m_H = 120$ GeV. Both figures are normalized to their asymptotic values given in Eq. (10).

III. $H \rightarrow gg$ AND $H \rightarrow \gamma\gamma$

The partial widths for $H \rightarrow gg$ and $H \rightarrow \gamma\gamma$ in the SM can be found in [11]. In general the partial widths can be expressed as

$$\begin{aligned} \Gamma(H \rightarrow gg) &= \frac{\alpha_s^2 m_H^3}{32\pi^3 v^2} \left| \sum_i -\frac{1}{2} y_i F_{1/2}(\tau_i) \right|^2 = \frac{\sqrt{2} G_F \alpha_s^2 m_H^3 y_{G_F}^2}{32\pi^3} \left| \sum_i -\frac{1}{2} y_i F_{1/2}(\tau_i) \right|^2, \\ \Gamma(H \rightarrow \gamma\gamma) &= \frac{\alpha^2 m_H^3}{256\pi^3 v^2} \left| \sum_i y_i N_{ci} Q_i^2 F_i \right|^2 = \frac{\sqrt{2} G_F \alpha^2 m_H^3 y_{G_F}^2}{256\pi^3} \left| \sum_i y_i N_{ci} Q_i^2 F_i \right|^2, \end{aligned} \quad (6)$$

where N_{ci} , Q_i are the color factor and electric charge respectively for a particle i running in the loop. The dimensionless loop factors for particles of spin given in the subscript are [11]

$$F_1 = 2 + 3\tau + 3\tau(2 - \tau)f(\tau), \quad F_{1/2} = -2\tau[1 + (1 - \tau)f(\tau)], \quad F_0 = \tau[1 - \tau f(\tau)], \quad (7)$$

with

$$f(\tau) = \begin{cases} [\sin^{-1}(1/\sqrt{\tau})]^2, & \tau \geq 1 \\ -\frac{1}{4}[\ln(\eta_+/\eta_-) - i\pi]^2, & \tau < 1 \end{cases} \quad (8)$$

and

$$\tau_i = 4M_i^2/m_H^2, \quad \eta_{\pm} = 1 \pm \sqrt{1 - \tau}. \quad (9)$$

In the limit of large τ , *i.e.*, when the particle in the loop is much heavier than H , the loop factors approach constant values:

$$F_1 \rightarrow 7, \quad F_{1/2} \rightarrow -4/3, \quad F_0 \rightarrow -1/3. \quad (10)$$

On the other hand, for $\tau < 1$ the loop factor develops an imaginary part after crossing the real production threshold of particle pairs in the loop. The loop functions normalized to their asymptotic values are shown in Fig. 2. $F_1(\tau_{W_L})$ and $F_{1/2}(\tau_t)$ are presented as a function of m_H in Fig. 2(a). They are just the SM results for the W and top-quark loops. The loop functions F_1 ,

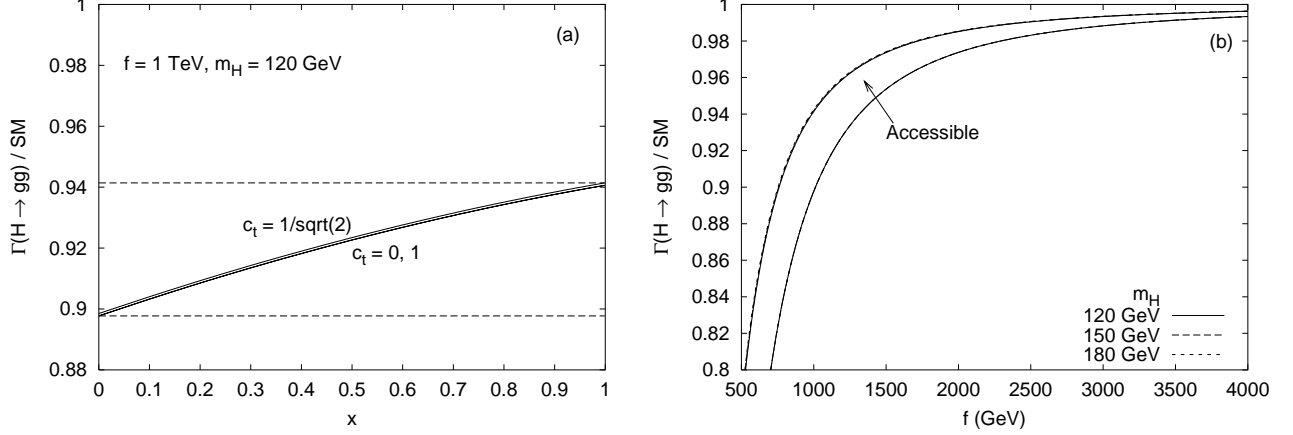


FIG. 3: (a) Dependence of $\Gamma(H \rightarrow gg)$ on the parameters x and c_t for $f = 1$ TeV and $m_H = 120$ GeV, normalized to the SM partial width. The solid lines show $\Gamma(H \rightarrow gg)/\text{SM}$ as a function of x for $c_t = 1$ or 0 and $1/\sqrt{2}$ (top to bottom). The dashed lines indicate the minimum ($c_t = 0$ or 1 , $x = 0$) and maximum ($c_t = 1/\sqrt{2}$, $x = 1$) values of $\Gamma(H \rightarrow gg)/\text{SM}$ obtainable in the LH model for $f = 1$ TeV. (b) Accessible range of $\Gamma(H \rightarrow gg)/\text{SM}$ in the LH model versus f for various values of m_H as indicated.

$F_{1/2}$ and F_0 for the heavy particles are shown in Fig. 2(b) versus the heavy particle mass. One can clearly see that the loop functions for the heavy particles are very close to their asymptotic values.

In Eq. (6), the coefficients y_i are the correction factors of the Higgs boson couplings with respect to the SM values. Expressing the resulting loop integrals as the dimensionless functions $F_1, F_{1/2}, F_0$, the fact that the SM couplings y_t, y_{W_L} are of order unity is because the Higgs boson couplings to t and W_L are proportional to their masses. This is not true for the heavy particles in the LH model, since they acquire their mass not from their coupling to H but rather from the f condensate. Consequently, all the corrections due to heavy particles in the loop are proportional to v^2/f^2 , as is evident from Eq. (4). This behavior naturally respects the decoupling limit for physics with much higher scale f .

A. $H \rightarrow gg$

In the LH model, the decay $H \rightarrow gg$ receives a contribution from the new heavy quark T . The partial width of $H \rightarrow gg$ is given explicitly by

$$\begin{aligned} \Gamma(H \rightarrow gg) &= \frac{\sqrt{2}G_F\alpha_s^2 m_H^3}{32\pi^3} \left| -\frac{1}{2}F_{1/2}(\tau_t)y_t y_{G_F} - \frac{1}{2}F_{1/2}(\tau_T)y_T \right|^2 \\ &= \frac{\sqrt{2}G_F\alpha_s^2 m_H^3}{32\pi^3} \left| -\frac{1}{2}F_{1/2}(\tau_t) - \frac{1}{2}\frac{v^2}{f^2} \left[\left(-\frac{7}{8} + \frac{1}{2}x - \frac{1}{8}x^2 \right) F_{1/2}(\tau_t) \right. \right. \\ &\quad \left. \left. + c_t^2 s_t^2 (F_{1/2}(\tau_t) - F_{1/2}(\tau_T)) \right] \right|^2. \end{aligned} \quad (11)$$

The first term in the absolute square is the SM result due to the top quark. Examining the correction terms in the square brackets, we see that the first term is negative for $0 \leq x < 1$,

leading to a suppression of $\Gamma(H \rightarrow gg)$ compared to its SM value. This term comes from y_{G_F} and from the terms in y_t independent of c_t [see Eq. (4)], which are due to the mixing in the Higgs sector and the effects of expanding out the fields of the nonlinear σ -model in the fermion mass terms. The second term in the square brackets, which arises from the T quark loop plus the mixing between the SM top quark and the new heavy vector-like quark, is positive but too small to counteract the negative first term. Note that in the limit that $m_t \rightarrow M_T$, $F_{1/2}(\tau_t) - F_{1/2}(\tau_T) \rightarrow 0$ and this second term vanishes. This is because H does not couple to the heavy vector-like quark in the gauge eigenstate basis, so the mixing becomes irrelevant as the masses become degenerate. Because $F_{1/2}$ approaches a constant at large τ and thus does not depend sensitively on f , the deviation of $\Gamma(H \rightarrow gg)$ from its SM value simply scales like $1/f^2$.

The dependence of $\Gamma(H \rightarrow gg)$ on x is shown in Fig. 3(a) for various values of c_t , normalized to the SM partial width. We first note that the LH corrections are always negative, mainly due to the reduced coupling strength of y_t , y_{G_F} . There is both linear and quadratic dependence on x , but the linear term has a larger coefficient by a factor of 4, as is evident from the solid curves in Fig. 3(a). The x -dependence leads to a reduction of the partial width varying between about 6 – 10% of the SM value for $f = 1$ TeV, as indicated by the range between the dashed lines. The c_t -dependence of the cross section, as shown by the range of the solid curves in the figure, is quite weak, leading to a variation of the partial width by less than 1% of the SM value for $f = 1$ TeV. This is due to the near-cancellation of the c_t -dependence between the t and T loops, as illustrated in Eq. (11). For instance, for $m_H = 120$ GeV, $F_{1/2}(\tau_t)/2 \simeq -0.686$ and $F_{1/2}(\tau_T)/2 \simeq -2/3$, so the term proportional to $c_t^2 s_t^2$ has a very small coefficient. To further explore the maximum variation to the SM prediction, we show the accessible range of LH corrections versus f for various m_H values in Fig. 3(b). The lower limit is independent of m_H because it is reached when $y_T = 0$. In this case, the amplitude is proportional to $F_{1/2}(\tau_t)$ only, so the m_H -dependence cancels in the ratio with the SM partial width. The upper limit depends on m_H since the T loop contributes, and $F_{1/2}(\tau_T)$ has a different m_H -dependence than $F_{1/2}(\tau_t)$. While the m_H -dependence is rather weak, we see that the reduction from the SM prediction can be significant. All of these features can be explicitly illustrated by examining the numerical coefficients after normalizing the partial width to its SM value as

$$\frac{\Gamma(H \rightarrow gg)}{\Gamma_{\text{SM}}(H \rightarrow gg)} = 1 + \left[-0.106 + 0.061x - 0.015x^2 + 0.003c_t^2 s_t^2 \right] \left(\frac{1 \text{ TeV}}{f} \right)^2, \quad (12)$$

where the m_H -dependence is only in the coefficient of the $c_t^2 s_t^2$ term; here we have chosen $m_H = 120$ GeV. Examining Eqs. (11) and (12), we see that the partial width reaches its maximum value (minimum deviation from the SM) at $x = 1$ and $c_t = 1/\sqrt{2}$, and reaches its minimum value (maximum deviation from the SM) at $x = 0$ and $c_t = 0$ or 1.

B. $H \rightarrow \gamma\gamma$

The decay $H \rightarrow \gamma\gamma$ in the LH model receives contributions from the new charged particles W_H^\pm , T , and Φ^\pm . The partial width is given by

$$\Gamma(H \rightarrow \gamma\gamma) = \frac{\sqrt{2}G_F\alpha^2 m_H^3}{256\pi^3} \left| \frac{4}{3}F_{1/2}(\tau_t)y_t y_{G_F} + \frac{4}{3}F_{1/2}(\tau_T)y_T + F_1(\tau_{W_L})y_{W_L}y_{G_F} \right|$$

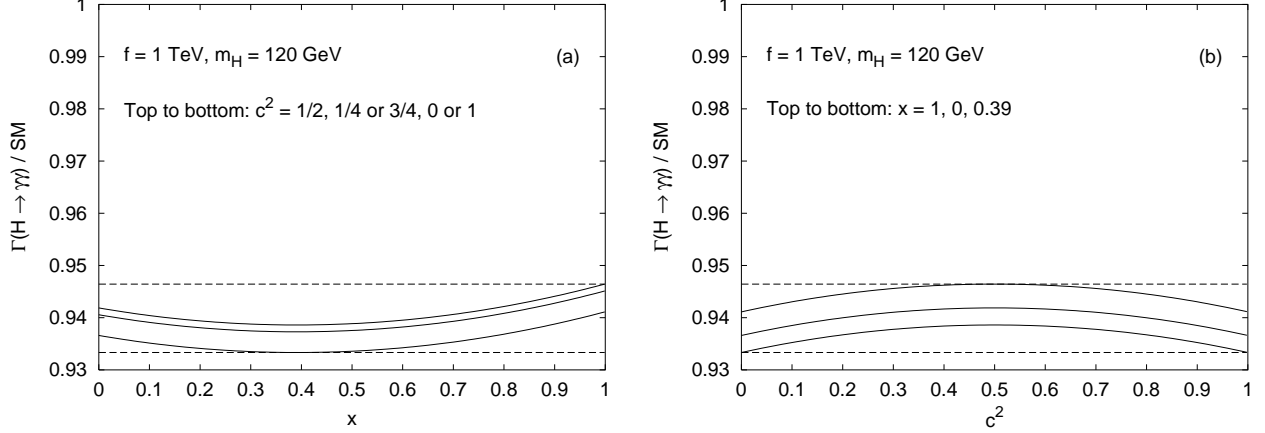


FIG. 4: Dependence of $\Gamma(H \rightarrow \gamma\gamma)$ on the model parameters for $f = 1$ TeV and $m_H = 120$ GeV, normalized to the SM partial width. The solid and short-dashed lines show $\Gamma(H \rightarrow \gamma\gamma)$ relative to its SM value as a function of x^2 for several values of c^2 (a) and as a function of c^2 for several values of x (b). The solid lines are for $c_t = 0$ and the short dashed lines are for $c_t = 1$. The long dashed lines show the minimum ($c = 1/\sqrt{2}$, $c_t = x = 1$) and maximum ($c = 0$ or 1 , $c_t = x = 0$) values of $\Gamma(H \rightarrow \gamma\gamma)$ obtainable in the LH model for this value of f . Doubling f reduces the deviation from 1 by a factor of four.

$$\begin{aligned}
& + F_1(\tau_{W_H})y_{W_H} + F_0(\tau_\Phi)y_{\Phi^+} \Big|^2 \\
& = \frac{\sqrt{2}G_F\alpha^2 m_H^3}{256\pi^3} \left| \frac{4}{3}F_{1/2}(\tau_t) + F_1(\tau_{W_L}) + \frac{v^2}{f^2} \left[\frac{4}{3} \left(-\frac{7}{8} + \frac{1}{2}x - \frac{1}{8}x^2 \right) F_{1/2}(\tau_t) \right. \right. \\
& \quad + \frac{4}{3}c_t^2 s_t^2 (F_{1/2}(\tau_t) - F_{1/2}(\tau_T)) + \left(-\frac{3}{8} - \frac{1}{4}(c^2 - s^2)^2 + \frac{1}{8}x^2 \right) F_1(\tau_{W_L}) \\
& \quad \left. \left. - s^2 c^2 F_1(\tau_{W_H}) + \left(-\frac{1}{3} + \frac{1}{4}x^2 \right) F_0(\tau_\Phi) \right] \right|^2. \tag{13}
\end{aligned}$$

The first two terms in the absolute square are the SM results from the top quark and W boson. For $m_H = 120$ GeV, $4F_{1/2}(\tau_t)/3 \simeq -1.83$ and $F_1(\tau_{W_L}) \simeq 8.17$. In general, for $m_H < 2M_{W_L}$, the loop function F_1 (for W_L and W_H) is real and positive, while the loop functions $F_{1/2}$ and F_0 (for t , T , and Φ^+) are real and negative. The amplitude is dominated by the contribution from W_L and is therefore positive.

The behavior of the contributions of t and T is exactly as in the case of $\Gamma(H \rightarrow gg)$. However, because fermion loops enter with a minus sign in $\Gamma(H \rightarrow \gamma\gamma)$, the effects in the t and T loops that lead to a suppression of $\Gamma(H \rightarrow gg)$ tend to *enhance* $\Gamma(H \rightarrow \gamma\gamma)$. The third term in the square brackets comes from y_{G_F} and y_{W_L} and is always negative. The term proportional to $(c^2 - s^2)^2$ comes from the mixing between W_L and W_H and suppresses the partial width. The W_H loop amplitude has a negative coefficient due to the $-g$ in the coupling of $W_H^+ W_H^- H$ (see Refs. [3, 7] for details), which tends to suppress the partial width. The last term in the square brackets is due to the Φ^+ loop; its negative coefficient leads to an enhancement of the amplitude, but because scalars suffer from the small loop factor of $F_0 \simeq -1/3$, its effect is insignificant. Again, the deviation of $\Gamma(H \rightarrow \gamma\gamma)$ from its SM value scales like $1/f^2$.

The dependence of $\Gamma(H \rightarrow \gamma\gamma)$ on the parameters c and x is illustrated in Fig. 4. The

deviation in $\Gamma(H \rightarrow \gamma\gamma)$ is almost quadratic in x as seen in Fig. 4(a). This is due to the dominant contribution from $F_1(\tau_{W_L})$ with the x^2 -dependent coefficients of y_{W_L} and y_{G_F} . Linear dependence on x enters via y_t ; however, this contribution is small because of the small top quark contribution compared to the W boson contribution. Varying x between 0 and 1 changes the partial width by as much as 0.8% of the SM prediction for $f = 1$ TeV. The partial width is also sensitive to the gauge mixing angle c , due to the W_L and W_H loops. It is quadratic in c^2 , as seen in Fig. 4(b). Varying c between $1/\sqrt{2}$ and 1 or 0 changes the partial width again by about 0.5% for $f = 1$ TeV. The partial width is almost independent of c_t because of the near-cancellation of the c_t -dependence between the t and T loops, as discussed earlier. The resulting accessible range of $\Gamma(H \rightarrow \gamma\gamma)$ is shown in Fig. 5. The effect can be quite significant.

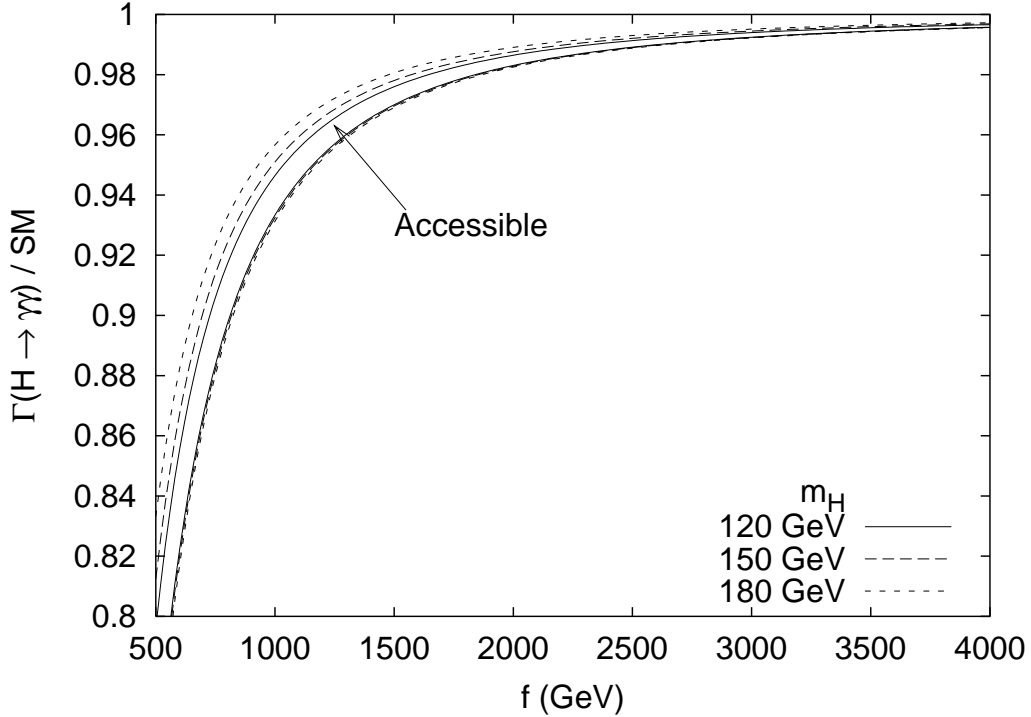


FIG. 5: Range of values of $\Gamma(H \rightarrow \gamma\gamma)$ accessible in the LH model as a function of f , normalized to the SM value, for $m_H = 120, 150$ and 180 GeV.

For instance, for $f = 1$ TeV, the deviation from the SM prediction can be $-(5 - 7\%)$. All of these features can be made explicit if we write the expression normalized to the SM partial width,

$$\frac{\Gamma(H \rightarrow \gamma\gamma)}{\Gamma_{\text{SM}}(H \rightarrow \gamma\gamma)} = 1 + \left[-0.0634 + 0.0211c^2s^2 - 0.0166x - 0.0211x^2 - 0.0009c_t^2s_t^2 \right] \left(\frac{1 \text{ TeV}}{f} \right)^2 \quad (14)$$

where we have chosen $m_H = 120$ GeV. All of the coefficients in the square brackets now depend on m_H .

To summarize the results of the partial width calculations, the values of c , c_t and x that minimize and maximize each partial width are given in Table I. We have also included the percentage decrease with respect to the SM predictions when varying the parameters from the maximum width to the minimum. Note that any colored states that enhance the $H \rightarrow gg$

| Parameter | $\Gamma(H \rightarrow gg)$ | | Percent Decrease | $\Gamma(H \rightarrow \gamma\gamma)$ | | Percent Decrease |
|-----------|----------------------------|----------|---------------------|--------------------------------------|--------------|---------------------|
| | Maximize | Minimize | | Maximize | Minimize | |
| c | — | — | — | $1/\sqrt{2}$ | 0 or 1 | 0.5% |
| x | 1 | 0 | 4% | 1 | 0.39 | 0.8% |
| c_t | $1/\sqrt{2}$ | 0 or 1 | 0.1% | 0 or 1 | $1/\sqrt{2}$ | negligible |

TABLE I: Parameters to maximize or minimize the partial widths, and the percent change between maximum and minimum (with respect to the SM values) for $f = 1$ TeV and $m_H = 120$ GeV. The percent change scales as $1/f^2$.

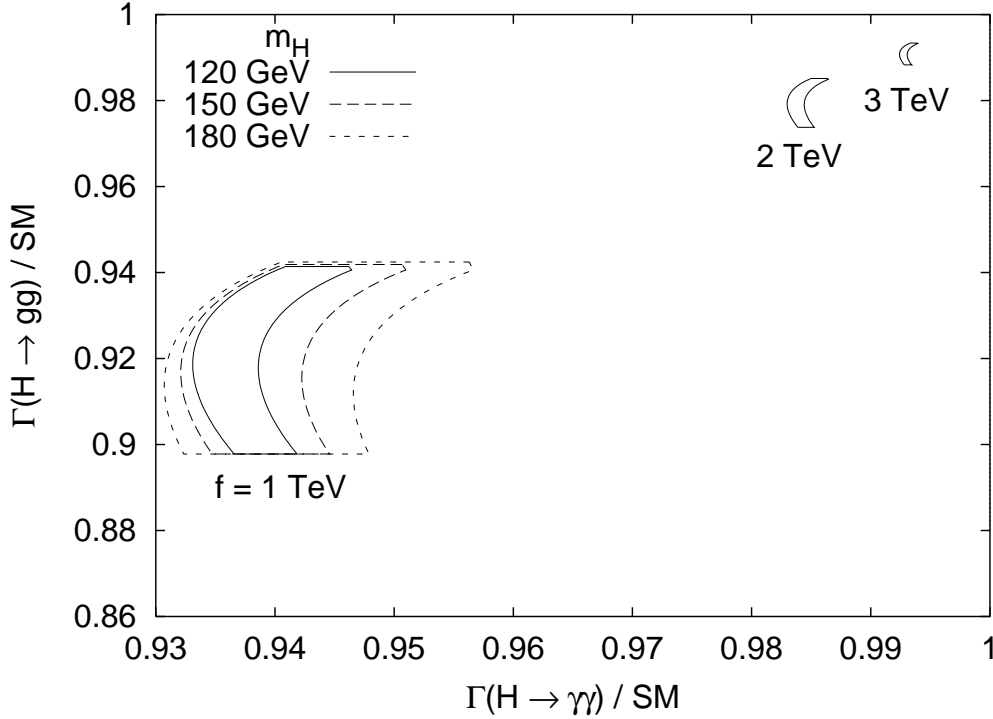


FIG. 6: Range of values of $\Gamma(H \rightarrow gg)$ versus $\Gamma(H \rightarrow \gamma\gamma)$ accessible in the LH model normalized to the SM value, for $m_H = 120, 150, 180$ GeV and for $f = 1, 2, 3$ TeV.

partial width would reduce the $H \rightarrow \gamma\gamma$ partial width. We illustrate the correlation between $\Gamma(H \rightarrow \gamma\gamma)$ and $\Gamma(H \rightarrow gg)$ in Fig. 6, where the accessible ranges for $f = 1, 2, 3$ TeV are presented. Also shown is the dependence on m_H for the case of $f = 1$ TeV.

C. Measurements of Higgs couplings to gg and $\gamma\gamma$

1. Higgs couplings at the LHC

The coupling of H to gg can be probed at the LHC through the cross section for Higgs production via gluon fusion. Taking the ratio of Higgs production rates from gluon fusion and from weak boson fusion with decays to common final states yields the ratio of partial widths $\Gamma(H \rightarrow gg)/\Gamma(H \rightarrow WW)$; the LHC can measure this ratio with a precision of 25 – 30%

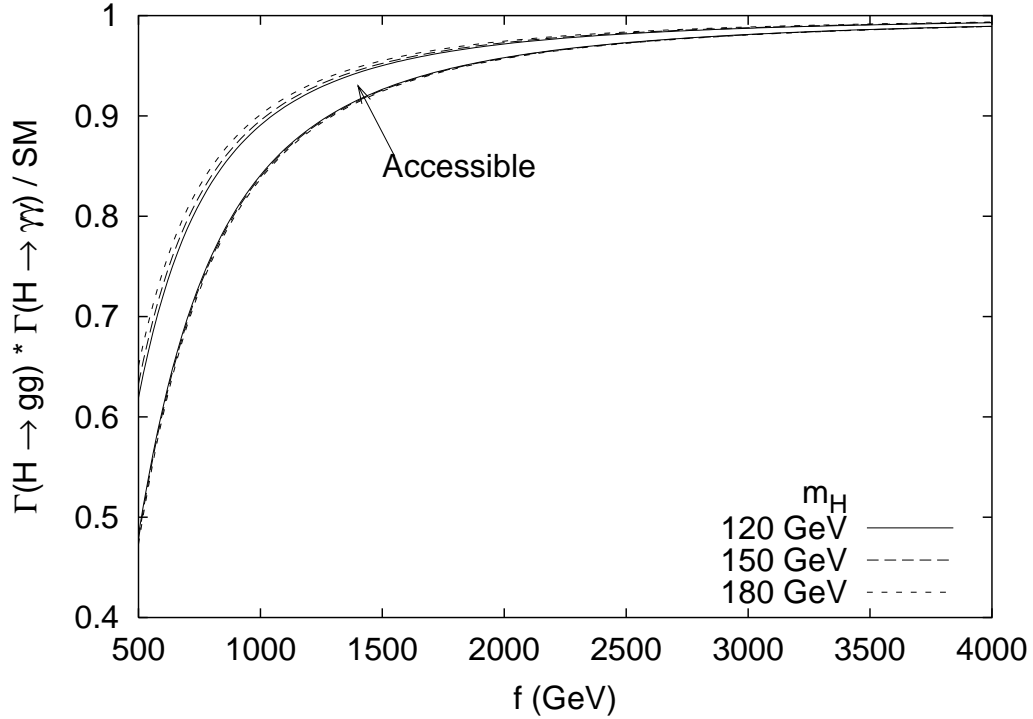


FIG. 7: Range of values of $\Gamma(H \rightarrow gg) \times \Gamma(H \rightarrow \gamma\gamma)$ accessible in the LH model as a function of f , normalized to the SM value, for $m_H = 120, 150$ and 180 GeV.

for $100 \text{ GeV} < m_H < 200 \text{ GeV}$ [13]. The partial width $\Gamma(H \rightarrow gg)$ can be extracted also with a precision of $25 - 30\%$ over this same range of m_H [13]. The SM partial decay width for $H \rightarrow gg$ has been computed accurately to the order of α_s^4 [14], and the production cross section for $gg \rightarrow H$ has been computed at next-to-next-to-leading order [10]. The remaining renormalization and factorization scale dependence of the cross section gives a lower bound on the theoretical uncertainty due to uncomputed higher order QCD corrections of about 15% . This large experimental and theoretical uncertainty may preclude the detection of the deviation of the LH model from the SM.

The coupling of H to $\gamma\gamma$ can be probed at the LHC through $H \rightarrow \gamma\gamma$, with H produced via gluon fusion or weak boson fusion. The rates for both $gg \rightarrow H \rightarrow \gamma\gamma$ and $VV \rightarrow H \rightarrow \gamma\gamma$ can be measured with a precision of $10 - 15\%$ for $m_H < 150 \text{ GeV}$ [13]. Taking ratios of rates as above but with common Higgs production mechanisms one can extract the ratio of partial widths $\Gamma(H \rightarrow \gamma\gamma)/\Gamma(H \rightarrow WW)$ with a precision of $10 - 20\%$ for $115 \text{ GeV} < m_H < 150 \text{ GeV}$ [13]. The partial width for $\Gamma(H \rightarrow \gamma\gamma)$ [15] can be extracted with a precision of $15 - 20\%$ over the same Higgs mass range [13]. Such a measurement gives a sensitivity only to $f < 650 \text{ GeV}$ at the 1σ level, which is still marginal to reach the possible new mass scale anticipated in the LH model.

As discussed in the previous section, we noticed the correlation between $\Gamma(H \rightarrow gg)$ and $\Gamma(H \rightarrow \gamma\gamma)$. Since a very promising channel for the Higgs search at the LHC is $gg \rightarrow H \rightarrow \gamma\gamma$, it is natural to ask how the product as a whole is affected. Figure 7 presents the accessible range for the product $\Gamma(H \rightarrow gg) \times \Gamma(H \rightarrow \gamma\gamma)$ versus f , normalized to the SM value. We see that the effect is to reduce the production rate with respect to the SM expectation, from -11% to -16% for $f = 1 \text{ TeV}$.

2. Higgs couplings at an e^+e^- collider

At an e^+e^- collider, the Higgs partial widths can be measured in a model-independent way. The technique involves tagging $e^+e^- \rightarrow Z^* \rightarrow ZH$ events using the Z recoil mass and counting final states, thus determining absolute branching fractions; $e^+e^- \rightarrow W^*W^* \rightarrow H\nu\bar{\nu}$ is then used to measure the HW^+W^- coupling to compute $\Gamma(H \rightarrow WW)$ and thus solve for the individual partial widths. The cross section for $e^+e^- \rightarrow ZH$ is largest at lower center-of-mass energies not too much above the ZH production threshold. The cross section for $e^+e^- \rightarrow H\nu\bar{\nu}$ grows with increasing center-of-mass energy and can thus be used at higher \sqrt{s} to increase the statistics. At higher energies, however, the H decay products are more highly boosted, making b , c and τ tagging more difficult.

The branching ratio of H into gg can be measured with a precision of about 6 – 20% at an e^+e^- collider [16, 17, 18]. $H \rightarrow gg$ is assumed to be what is left over after the $b\bar{b}$, $c\bar{c}$ and $\tau\tau$ final states are subtracted off of $H \rightarrow \text{jets}$. This measurement clearly depends on excellent charm tagging and varies depending on detector design and machine energy. As in $gg \rightarrow H$ at the LHC, the theoretical uncertainty in the SM prediction is likely of order 15% from uncalculated higher order QCD corrections [10, 14]. Such a measurement would thus be sensitive only to $f < 600$ GeV at the 1σ level.

The measurement of the branching ratio of $H \rightarrow \gamma\gamma$ at an e^+e^- collider is limited by low statistics due to the small $H \rightarrow \gamma\gamma$ branching ratio $\sim 10^{-3}$. With 500 fb^{-1} of integrated luminosity one can expect a precision of about 15 – 20% on the branching ratio and the same for the partial width [16, 17, 19]. This measurement would be sensitive to $f < 650$ GeV at the 1σ level, comparable to the sensitivity at the LHC.

3. Higgs couplings at a photon collider

A photon collider can produce the Higgs resonance in the s -channel with a cross section proportional to $\Gamma(H \rightarrow \gamma\gamma)$. For a light Higgs boson with mass around 115 – 120 GeV, the most precisely measured rate will be $\gamma\gamma \rightarrow H \rightarrow b\bar{b}$, with a precision of about 2% [20]. (The uncertainty rises to 10% for $m_H = 160$ GeV.) This can be combined with the measurement of the branching ratio of $H \rightarrow b\bar{b}$ measured to about 2% at the e^+e^- collider [16, 17, 18] to extract $\Gamma(H \rightarrow \gamma\gamma)$ with a precision of about 3%. Such a measurement would be sensitive to $f < 1500$ GeV at the 1σ level, or $f < 1100$ GeV at the 2σ level. A 5σ deviation is possible for $f < 700$ GeV.

IV. DISCUSSION AND CONCLUSIONS

New physics must enter the theory at the cutoff scale $\Lambda \simeq 4\pi f$ to complete the non-linear σ -model into a linear model. Because the processes $H \rightarrow gg$ and $H \rightarrow \gamma\gamma$ are finite at the leading one-loop order, they do not receive an arbitrarily large renormalization from cutoff-scale physics. However, this new physics will generically contain additional charged or colored fields that can run in the loop, leading to additional contributions to $H \rightarrow gg$ and $H \rightarrow \gamma\gamma$. We can estimate their size as follows. We focus on $H \rightarrow \gamma\gamma$, but similar conclusions can be drawn for $H \rightarrow gg$. The largest contributions will generically come from new gauge bosons, since their loop factor F_1 is the largest in the asymptotic limit. Consider a single charged gauge boson

with mass of order Λ and coupling to H of g_Λ . Its contribution to the amplitude will be smaller by a factor of $g_\Lambda^2(f^2/\Lambda^2)$ than the contribution from W_H , as can be estimated by an argument of explicit loop calculations or using the Naive Dimensional Analysis [21]. As long as $g_\Lambda < 4\pi$, the new physics at the scale Λ will not significantly change our conclusions, unless there is a large multiplicity of new particles that couple to H .

While the LH model that we have studied here contains only a single light Higgs doublet, many little Higgs models in the literature contain two light Higgs doublets [2]. The low-energy theory of these models is therefore a two Higgs doublet model (2HDM), containing a light charged Higgs boson H^\pm that can run in the loop in addition to the new particles at the scale f . Assuming that the dimensionless Higgs self-coupling $\lambda_{H^\pm H^\mp H}$ in the 2HDM is of order one as is natural, a relatively light H^\pm with a mass of $100 - 150$ GeV can have quite a sizable effect on $\Gamma(H \rightarrow \gamma\gamma)$ of $15 - 40\%$ times $\lambda_{H^\pm H^\mp H}$. For a heavier H^\pm above 300 GeV, the deviation is below 5% . Potentially more important than the H^\pm loop, however, is the effect of mixing between the neutral components of the two Higgs doublets. This mixing can affect the couplings of H to W_L and t in a very significant way if the second Higgs doublet is relatively light, leading to large deviations in $\Gamma(H \rightarrow gg)$ and $\Gamma(H \rightarrow \gamma\gamma)$. If the dimensionless Higgs self-couplings are again of order one, the deviation of the $HW_L^+W_L^-$ coupling from its SM value due to 2HDM mixing is of order m_Z^2/m_A^2 and that of the $Ht\bar{t}$ coupling is of order m_Z/m_A , where m_A is the mass scale of the heavier Higgs doublet (more precisely, m_A is the mass of the pseudoscalar Higgs boson A^0). For additional details, see Ref. [11]. These deviations are thus generically larger than the deviations due to the heavy states at the scale f .

In conclusion, our results are robust in little Higgs models that contain only a single light Higgs boson. The dominant contributions to the deviations of $\Gamma(H \rightarrow gg)$ and $\Gamma(H \rightarrow \gamma\gamma)$ from their SM values are due to (i) the new T quark and W_H bosons in the loop, which contribute at the order v^2/f^2 since they get their masses from the condensate f ; and (ii) the modification of the $t\bar{t}H$ and $W_L^+W_L^-H$ couplings due to mixing with the heavy states, which also contributes at order v^2/f^2 . Any little Higgs model must contain such a heavy T and W_H with masses of order f to cancel the quadratic divergence of m_H due to the top quark and W_L , and these new heavy states will generically mix with the corresponding SM particles at order v^2/f^2 . Therefore the gross features of our analysis should carry over.

To summarize, we found that for $f = 1$ TeV, $\Gamma(H \rightarrow gg)$ is reduced by $6 - 10\%$ in the LH model compared to its SM value, where the variation is mainly due to the dependence on x , while $\Gamma(H \rightarrow \gamma\gamma)$ is reduced by $5 - 7\%$ of its SM value, where the variation is mainly due to the dependence on x and c . The deviations scale with $1/f^2$. A photon collider could probe the deviation in $\Gamma(H \rightarrow \gamma\gamma)$ up to $f \lesssim 1.5$ TeV (1.1 TeV, 0.7 TeV) at the 1σ (2σ , 5σ) level.

Note added: When the current paper was being completed, another paper on a similar subject appeared [22]. In calculating the Higgs decay widths, the authors of Ref. [22] did not take into account mixing and interference effects between the SM particles and the new heavy states, and thus reached negligibly small results of the order $(v/f)^4$.

Acknowledgments

This work was supported in part by the U.S. Department of Energy under grant DE-FG02-95ER40896 and in part by the Wisconsin Alumni Research Foundation.

APPENDIX A

Here we present some details of the Higgs sector of the LH model and derive the $H\Phi^+\Phi^-$ and $H\Phi^{++}\Phi^{--}$ couplings.

The most general scalar potential invariant under the Standard Model gauge groups involving one doublet field h and one triplet field ϕ can be written up to operators of dimension four as:

$$V = \lambda_{\phi^2} f^2 \text{Tr}(\phi^\dagger \phi) + i\lambda_{h\phi h} f (h\phi^\dagger h^T - h^* \phi h^\dagger) - \mu^2 h h^\dagger + \lambda_{h^4} (h h^\dagger)^2 \\ + \lambda_{h\phi\phi h} h\phi^\dagger \phi h^\dagger + \lambda_{h^2\phi^2} h h^\dagger \text{Tr}(\phi^\dagger \phi) + \lambda_{\phi^2\phi^2} (\text{Tr}(\phi^\dagger \phi))^2 + \lambda_{\phi^4} \text{Tr}(\phi^\dagger \phi \phi^\dagger \phi). \quad (\text{A1})$$

The coefficients in this potential are constrained by the symmetries of the Littlest Higgs model. At tree-level, there is no Higgs potential. A Coleman-Weinberg potential is generated after the heavy gauge bosons and vector-like quark are integrated out. The quadratically divergent terms of the one-loop Coleman-Weinberg potential each preserve one of two global $SU(3)$ symmetries, while breaking the other (see Ref. [3] for details).

From the quadratically divergent part of the one-loop Coleman-Weinberg potential, we have:

$$\lambda_{\phi^2} = \frac{a}{2} \left[\frac{g^2}{s^2 c^2} + \frac{g'^2}{s'^2 c'^2} \right] + 8a' \lambda_1^2, \\ \lambda_{h\phi h} = -\frac{a}{4} \left[g^2 \frac{(c^2 - s^2)}{s^2 c^2} + g'^2 \frac{(c'^2 - s'^2)}{s'^2 c'^2} \right] + 4a' \lambda_1^2, \\ \lambda_{h^4} = \frac{1}{4} \lambda_{\phi^2}, \quad \lambda_{h\phi\phi h} = -\frac{4}{3} \lambda_{\phi^2}, \quad \lambda_{\phi^2\phi^2} = -16a' \lambda_1^2, \\ \lambda_{\phi^4} = -\frac{2a}{3} \left[\frac{g^2}{s^2 c^2} + \frac{g'^2}{s'^2 c'^2} \right] + \frac{16a'}{3} \lambda_1^2, \quad (\text{A2})$$

where a and a' are unknown coefficients of order one that parameterize the effects of the UV-completion at the cutoff scale Λ .

The coefficients μ^2 and $\lambda_{h^2\phi^2}$ get no contribution from the quadratically divergent part of the one-loop Coleman-Weinberg potential because they are protected by *both* of the global $SU(3)$ symmetries of the LH model. Thus they receive only log-divergent contributions at one-loop, and quadratically divergent contributions at the two-loop level. The suppression of μ^2 from the extra loop factor gives the natural hierarchy between the electroweak scale and the cutoff scale Λ . Because $\lambda_{h^2\phi^2}$ is also generated at this order, it is not of order one like the other quartic couplings, but rather suppressed by $1/16\pi^2 \sim 10^{-2}$ and can be neglected for our purposes.

The $H\Phi^+\Phi^-$ coupling is given by the following terms in the interaction Lagrangian:

$$-\mathcal{L} = i\sqrt{2}\lambda_{h\phi h}(h^+ h^0 \phi^- - h^- h^{0*} \phi^+)f + \frac{1}{2}\lambda_{h\phi\phi h}\phi^+ \phi^- h^0 h^{0*} + \dots, \quad (\text{A3})$$

where the dots represent terms that give subleading contributions. Using the expressions for the couplings [7],

$$\lambda_{h\phi h} = \frac{xM_\Phi^2}{2f^2}, \quad \lambda_{h\phi\phi h} = -\frac{4M_\Phi^2}{3f^2}, \quad (\text{A4})$$

and the mixing angles between the gauge and mass eigenstates given in Ref. [7], we get for the $H\Phi^+\Phi^-$ coupling,

$$-\mathcal{L} = H\Phi^+\Phi^- \left[\frac{x^2 v}{2} - \frac{2v}{3} \right] \frac{M_\Phi^2}{f^2}. \quad (\text{A5})$$

The $H\Phi^{++}\Phi^{--}$ coupling is given by the following terms in the interaction Lagrangian:

$$-\mathcal{L} = 2\lambda_{\phi^2\phi^2}\phi^{++}\phi^{--}\phi^0\phi^{0*} + \lambda_{h^2\phi^2}\phi^{++}\phi^{--}h^0h^{0*} + \dots, \quad (\text{A6})$$

where again the dots represent terms that give subleading contributions. In terms of the mass eigenstates,

$$-\mathcal{L} = H\Phi^{++}\Phi^{--} \left[v \times \mathcal{O}(v'^2/v^2, 1/16\pi^2) \right]. \quad (\text{A7})$$

The $H\Phi^{++}\Phi^{--}$ coupling is thus highly suppressed relative to the $H\Phi^+\Phi^-$ coupling.

-
- [1] K. Hagiwara *et al.* [Particle Data Group Collaboration], Phys. Rev. D **66**, 010001 (2002).
 - [2] N. Arkani-Hamed, A. G. Cohen, and H. Georgi, Phys. Lett. B **513**, 232 (2001) [[arXiv:hep-ph/0105239](#)]; N. Arkani-Hamed, A. G. Cohen, T. Gregoire, and J. G. Wacker, JHEP **0208**, 020 (2002) [[arXiv:hep-ph/0202089](#)]; N. Arkani-Hamed, A. G. Cohen, E. Katz, A. E. Nelson, T. Gregoire, and J. G. Wacker, JHEP **0208**, 021 (2002) [[arXiv:hep-ph/0206020](#)]; I. Low, W. Skiba, and D. Smith, Phys. Rev. D **66**, 072001 (2002) [[arXiv:hep-ph/0207243](#)]; D. E. Kaplan and M. Schmaltz, [arXiv:hep-ph/0302049](#); For a recent review, see *e.g.*, M. Schmaltz, [arXiv:hep-ph/0210415](#).
 - [3] N. Arkani-Hamed, A. G. Cohen, E. Katz, and A. E. Nelson, JHEP **0207**, 034 (2002) [[arXiv:hep-ph/0206021](#)].
 - [4] S. R. Coleman and E. Weinberg, Phys. Rev. D **7**, 1888 (1973).
 - [5] C. Csaki, J. Hubisz, G.D. Kribs, P. Meade, and J. Terning, [arXiv:hep-ph/0211124](#);
 - [6] J.L. Hewett, F.J. Petriello, and T.G. Rizzo, [arXiv:hep-ph/0211218](#).
 - [7] T. Han, H. E. Logan, B. McElrath, and L. T. Wang, [arXiv:hep-ph/0301040](#).
 - [8] G. Burdman, M. Perelstein, and A. Pierce, [arXiv:hep-ph/0212228](#).
 - [9] S. Dawson, Nucl. Phys. **B359**, 283 (1991); A. Djouadi, M. Spira, and P.M. Zerwas, Phys. Lett. **B264**, 440 (1991); D. Graudenz, M. Spira, and P.M. Zerwas, Phys. Rev. Lett. **70**, 1372 (1993).
 - [10] R. V. Harlander and W. Kilgore, Phys. Rev. Lett. **88**, 201801 (2002), [[arXiv:hep-ph/0201206](#)]; C. Anastasiou and K. Melnikov, Nucl. Phys. **B646**, 220 (2002), [[arXiv:hep-ph/0207004](#)].
 - [11] J. F. Gunion, H. E. Haber, G. L. Kane, and S. Dawson, “The Higgs Hunter’s Guide,” Addison-Wesley, Reading, MA (1990).
 - [12] R. Martinez, M. A. Perez, and J. J. Toscano, Phys. Rev. D **40**, 1722 (1989).
 - [13] D. Zeppenfeld, in *Proc. of the APS/DPF/DPB Summer Study on the Future of Particle Physics (Snowmass 2001)* ed. N. Graf, eConf **C010630**, P123 (2001) [[arXiv:hep-ph/0203123](#)]; D. Zeppenfeld, R. Kinnunen, A. Nikitenko, and E. Richter-Was, Phys. Rev. D **62**, 013009 (2000) [[arXiv:hep-ph/0002036](#)]; A. Belyaev and L. Reina, JHEP **0208**, 041 (2002) [[arXiv:hep-ph/0205270](#)].
 - [14] K.G. Chetyrkin, Bernd A. Kniehl, and M. Steinhauser, Phys. Rev. Lett. **79**, 353 (1997) [[arXiv:hep-ph/9705240](#)]; Nucl. Phys. **B490**, 19 (1997) [[arXiv:hep-ph/9701277](#)].

- [15] H. Zheng and D. Wu, Phys. Rev. D **42**, 3760 (1990); A. Djouadi, M. Spira, J. J. van der Bij, and P. M. Zerwas, Phys. Lett. B **257**, 187 (1991); S. Dawson and R. P. Kauffman, Phys. Rev. D **47**, 1264 (1993); A. Djouadi, M. Spira, and P. M. Zerwas, Phys. Lett. B **311**, 255 (1993); K. Melnikov and O. I. Yakovlev, Phys. Lett. B **312**, 179 (1993) [[arXiv:hep-ph/9302281](#)]; M. Inoue, R. Najima, T. Oka, and J. Saito, Mod. Phys. Lett. A **9**, 1189 (1994); J. Fleischer and O. V. Tarasov, Z. Phys. C **64**, 413 (1994) [[arXiv:hep-ph/9403230](#)]; For a recent review, see *e.g.*, B. A. Kniehl, Int. J. Mod. Phys. A **17**, 1457 (2002) [[arXiv:hep-ph/0112023](#)].
- [16] T. Abe *et al.* [American Linear Collider Working Group], “Linear collider physics resource book for Snowmass 2001. 2: Higgs and supersymmetry studies,” in *Proc. of the APS/DPF/DPB Summer Study on the Future of Particle Physics (Snowmass 2001)* ed. N. Graf, [arXiv:hep-ex/0106056](#).
- [17] J. A. Aguilar-Saavedra *et al.* [ECFA/DESY LC Physics Working Group Collaboration], “TESLA Technical Design Report Part III: Physics at an e^+e^- Linear Collider,” [arXiv:hep-ph/0106315](#).
- [18] K. Abe *et al.* [ACFA Linear Collider Working Group Collaboration], “Particle physics experiments at JLC,” [arXiv:hep-ph/0109166](#).
- [19] E. Boos, J. C. Brient, D. W. Reid, H. J. Schreiber, and R. Shanidze, Eur. Phys. J. C **19**, 455 (2001) [[arXiv:hep-ph/0011366](#)].
- [20] D. Asner *et al.*, [arXiv:hep-ex/0111056](#); M. M. Velasco *et al.*, in *Proc. of the APS/DPF/DPB Summer Study on the Future of Particle Physics (Snowmass 2001)* ed. N. Graf, eConf **C010630**, E3005 (2001) [[arXiv:hep-ex/0111055](#)]; G. Jikia and S. Soldner-Rembold, Nucl. Phys. Proc. Suppl. **82**, 373 (2000) [[arXiv:hep-ph/9910366](#)]; Nucl. Instrum. Meth. A **472**, 133 (2001) [[arXiv:hep-ex/0101056](#)].
- [21] A. Manohar and H. Georgi, Nucl. Phys. B **234**, 189 (1984); H. Georgi, Phys. Lett. B **298**, 187 (1993) [[arXiv:hep-ph/9207278](#)].
- [22] C. Dib, R. Rosenfeld, and A. Zerwekh, [arXiv:hep-ph/0302068 v2](#).